



Exploring the biosynthetic capacity of TsrM, a B12-dependent Radical SAM Enzyme Catalyzing Non-radical Reactions

Feryel Soualmia, Alain Guillot, Nazarii Sabat, Clémence Brewée, Xavier Kubiak, Michael Haumann, Xavier Guinchard, Alhosna Benjdia, Olivier Berteau

► To cite this version:

Feryel Soualmia, Alain Guillot, Nazarii Sabat, Clémence Brewée, Xavier Kubiak, et al.. Exploring the biosynthetic capacity of TsrM, a B12-dependent Radical SAM Enzyme Catalyzing Non-radical Reactions. *Chemistry - A European Journal*, 2022, 28 (31), pp.e202200627. 10.1002/chem.202200627 . hal-03620811

HAL Id: hal-03620811

<https://hal.science/hal-03620811>

Submitted on 8 Nov 2022

HAL is a multi-disciplinary open access archive for the deposit and dissemination of scientific research documents, whether they are published or not. The documents may come from teaching and research institutions in France or abroad, or from public or private research centers.

L'archive ouverte pluridisciplinaire **HAL**, est destinée au dépôt et à la diffusion de documents scientifiques de niveau recherche, publiés ou non, émanant des établissements d'enseignement et de recherche français ou étrangers, des laboratoires publics ou privés.

Exploring the biosynthetic capacity of TsrM, a B₁₂-dependent Radical SAM Enzyme Catalyzing Non-radical Reactions

Feryel Soualmia,^[a] Alain Guillot,^[a] Nazarii Sabat,^[b] Clémence Brewée,^[a] Xavier Kubiak,^[a] Michael Haumann,^[c] Xavier Guinchard,^[b] Alhosna Benjdia,^{*[a]} Olivier Berteau,^{*[a]}

[a] Dr F. Soualmia, A. Guillot, C. Brewée, Dr X. Kubiak, Dr A. Benjdia, Dr. O Berteau
Micalis Institute, ChemSyBio
Université Paris-Saclay, INRAE, AgroParisTechd
78350, Jouy-en-Josas, France
E-mail: Olivier.berteau@inrae.fr, Alhosna.benjdia@inrae.fr

[b] Dr N. Sabat, Dr X. Guinchard
UPR 2301
Université Paris-Saclay, CNRS, Institut de Chimie des Substances Naturelles
91198, Gif-sur-Yvette, France

[c] Dr Michael Haumann
Department of Physics
Freie Universität Berlin
Arnimallee 14, 14195 Berlin, Germany

Abstract: B₁₂-dependent radical SAM enzymes are an emerging enzyme family with approximately 200,000 proteins. These enzymes have been shown to catalyze chemically challenging reactions such as methyl transfer to *sp*²- and *sp*³-hybridized carbon atoms. However, to date we have little information regarding their complex mechanisms and their biosynthetic potential. Here we show, using X-ray absorption spectroscopy, mutagenesis and synthetic probes that the vitamin B₁₂-dependent radical SAM enzyme TsrM can catalyze not only C- but also N-methyl transfer reactions further expanding its synthetic versatility. We also demonstrate that TsrM has the unique ability to directly transfer a methyl group to the benzyl core of tryptophan, including the least reactive position C4. Collectively, our study supports that TsrM catalyzes non-radical reactions and establishes the usefulness of radical SAM enzymes for novel biosynthetic schemes including serial alkylation reactions at particularly inert C-H bonds.

Introduction

More than 700,000 radical SAM enzymes are present within current genomic and metagenomics databases^[1]. These enzymes, which catalyze an unsurpassed diversity of reactions, are particularly abundant in the biosynthetic pathways of the so-called ribosomally synthesized and post-translationally modified peptides (RiPPs).^[1-2] In RiPPs, radical SAM enzymes have been shown to install chemically unprecedented post-translational modifications including epimerization,^[2d, 3] complex rearrangements,^[4] carbon-carbon^[5], and thioether bond formation^[2b, 2c, 6] as well as C-methylations.^[2g, 7] Despite this chemical versatility, the vast majority of known radical SAM enzymes uses S-adenosyl L-methionine (SAM) and an iron-sulfur cluster to activate their substrates and initiate radical reactions^[1a]. Among radical SAM enzymes, one of the largest group, with more than 200,000 proteins, is the vitamin B₁₂ (cobalamin)-dependent radical SAM enzymes^[8]. They are involved in the biosynthesis of myriad natural products from bacteriochlorophyll to antibiotics^[1a]. Notably, they have been shown to catalyze *P*-methylation^[9], ring contraction^[10] and C-methylation,^[7a, 7c, 8, 11] this latter modification being by far the most widespread in this group^[8]. Importantly, B₁₂-dependent radical SAM enzymes are the only known biological catalysts able to form carbon-carbon bonds between unactivated *sp*³-hybridized C-atoms^[7a, 8, 11a]. However, in the biosynthesis of thioestrepton A, a thiopeptide antibiotic with anti-cancer properties (Fig. 1)^[12], one B₁₂-dependent radical SAM enzymes TsrM, was shown to alkylate the C2-indolic position in L-tryptophan^[7c], an *sp*²-hybridized carbon atom. At odd with other known radical SAM enzymes, we have shown that during catalysis, TsrM neither produces 5'-deoxyadenosine (5'-dA), the by-product resulting from the homolytic cleavage of SAM, nor requires an external electron source for catalysis,^[7b, 7c] questioning the nature of the catalyzed reaction. Recently, the structure of an homolog of TsrM (*k*_sTsrM) was solved^[13] and it was shown that the radical SAM [4Fe4S] cluster was

fully coordinated by protein residues, proposed to hamper radical chemistry.

To gain insights into TsrM mechanism, we performed the first X-ray absorption spectroscopy (XAS) study of a B₁₂-dependent radical SAM enzyme and developed synthetic probes to explore its reactivity and synthetic potential.^[7b] Our results support that TsrM activity spans from the C2 to the C4 of tryptophan, the least reactive site of the indole system which can be activated only by a limited number of synthetic catalysts^[14] and indirectly by few biosynthetic systems.^[15] Unexpectedly, we also discovered that TsrM can efficiently transfer methyl groups not only to C-atoms, but also to nucleophilic nitrogen atoms expanding the mechanistic and catalytic repertoire of radical SAM enzymes. Collectively, our study establish TsrM as a unique and powerful biocatalysts for the facile and multi-alkylation of tryptophan/tryptamine derivatives and that it catalyzes non-radical reactions.

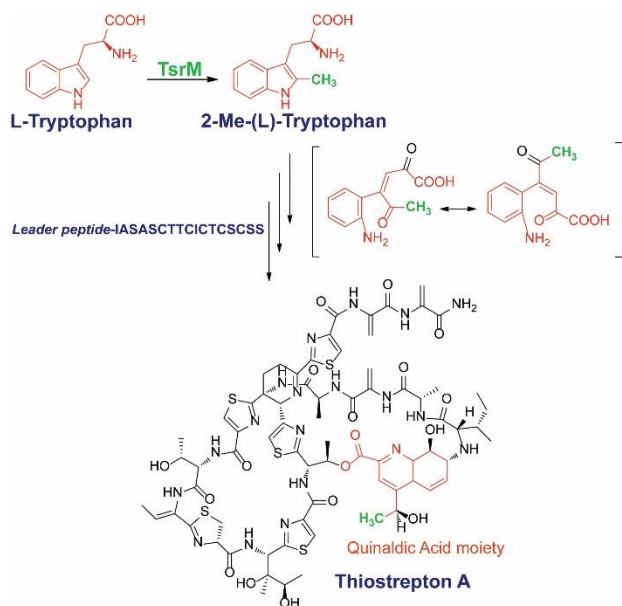


Figure 1. Thiostrepton biosynthetic pathway. The thiostrepton biosynthetic pathway requires more than 20 enzymes. TsrM catalyzes a key methyl transfer reaction on the C2-indolic position of L-tryptophan, the first step in the biosynthesis of the quinaldic moiety (indicated in red in the Thiostrepton A structure).

Results and Discussion

TsrM was recombinantly expressed in *E. coli* harboring an inducible *btuB* gene, responsible for B₁₂ import.^[16] When co-expressed in *E. coli* BL21, in the presence of hydroxycobalamin (OHCbl), TsrM was loaded with adenosylcobalamin (AdoCbl) because of the activity of the cobalamin adenosyltransferase BtuR. To prevent AdoCbl formation, we used an *E. coli* K12 Δ BtuR strain and obtained TsrM loaded only with OHCbl (**OHCbl-TsrM**). Contrary to recent report, we found no difference for the efficient production of cobalamin-loaded TsrM between the co-expression with BtuB alone or with the other vitamin B₁₂ import components: BtuC, D and F.^[17] To probe for the role of the radical SAM [4Fe-4S] cluster, we also generated a mutant (**A3-mutant**) in which the three cysteine residues involved in [4Fe-4S] cluster coordination (*i.e.* C253, C257 and C260), were replaced by alanine residues.

UV-visible analysis of OHCbl-TsrM (**Fig. 2**) was consistent with a previously published spectrum of TsrM expressed in ethanolamine-M9 medium, although we did not performed anaerobic iron-sulfur cluster reconstitution.^[18] This spectrum showed the contributions from both the cobalamin cofactor and the iron-sulfur cluster. In contrast, the **OHCbl-A3-mutant**, devoid of the iron-sulfur cluster, exhibited a typical OHCbl spectrum (**Fig. 2b**, inset) with absorption maxima at 350, 410, 509 and 538 nm. However, the similar A₃₅₀/A₂₈₀ ratio between the wild-type and **A3-mutant** supported that both enzymes contained similar amounts of bound cobalamin.

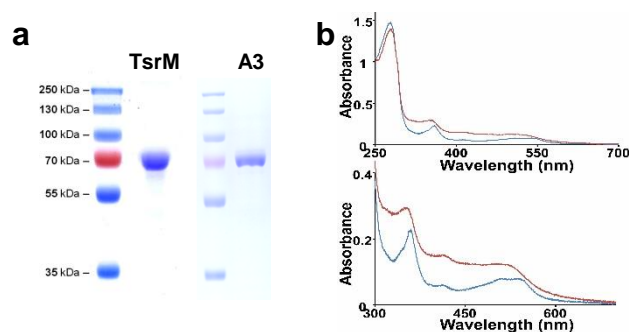


Figure 2. Purification and UV-visible spectrum of OHCbl-TsrM and OHCbl-A3 mutant. (a) Gel electrophoresis analysis. MW: molecular weight markers. (b) Upper panel: UV-visible spectrum of OHCbl-TsrM WT (red trace) and the OHCbl-A3-mutant (blue trace). Lower panel, zoom from 300 to 700 nm.

XAS analysis of TsrM. XAS spectra at the Co K-edge were collected on protein samples frozen under anaerobic conditions. We took advantage of our various expression systems to derive TsrM with bound OHCbl, AdoCbl, or methylcobalamin (MeCbl) cofactors. In all cases, the nature of the bound cobalamin cofactor was verified by HPLC analysis (**Supplementary Fig. S1**).

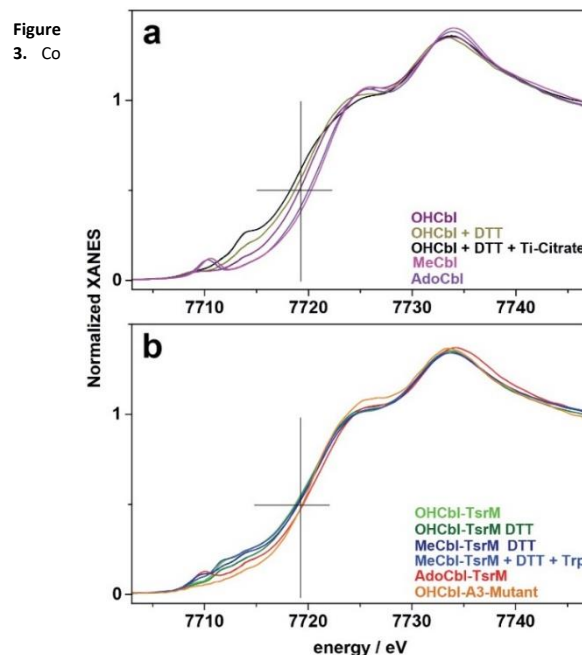


Figure 3. Co K-edge XANES spectra. (a) Cbl reference compounds: MeCbl, AdoCbl, and OHCbl in the absence or the presence of DTT or Ti-Citrate. (b) TsrM protein with bound Cbl. Black lines mark the K-edge half-height used for energy determination.

The Co K-edge spectra of the three forms (OHCbl-, AdoCbl- & MeCbl-TsrM) showed typical shapes for corrin-bound cobalt (Fig. 3). When reducing agents with increasing reduction potentials (*i.e.* DTT and Ti(III)Citrate) were added, the K-edge shifted to increasingly lower energies and the gradually emerging edge shoulder (~ 7714 eV) indicated increasing Co reduction and decreasing ligand numbers at the metal (Fig. 4).

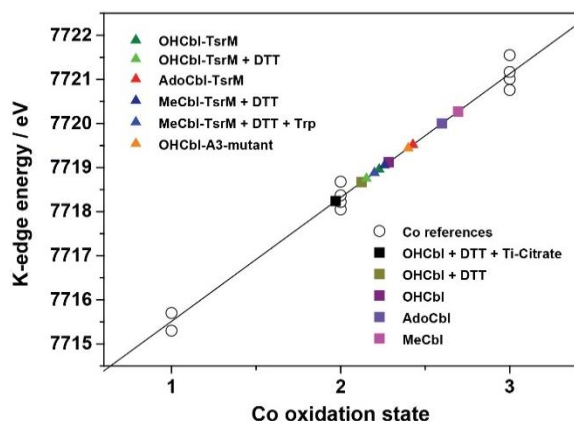


Figure 4. Co K-edge energies of OHCbl, AdoCbl and MeCbl-TsrM proteins. Co references (open circles) correspond to non-Cbl compounds described previously.^[19] The line is a fit to the reference compounds. Data points for the Cbl systems were placed on the fit line for the reference compounds.

For **OHCbl-TsrM**, the K-edge energy suggested similar amounts of Co(III) than for OHCbl in solution, meaning that DTT did not significantly reduce TsrM bound OHCbl. The more pronounced edge shoulder for **OHCbl-TsrM** vs solution OHCbl (Fig. 3b) suggested a base-off conformation of the cofactor in the protein (*i.e.* larger contributions from 5-coordinated Co(II)), consistent with a previous EPR analysis.^[18]

For **MeCbl-TsrM**, the pronounced pre-edge feature was consistent with methyl group binding at least at Co(III) and the edge shoulder supported a base-off cofactor, similar to **OHCbl-TsrM**. However, more Co(II) was found, suggesting a greater susceptibility to reduction. In the presence of DTT, SAM and tryptophan (Trp), minor changes in the low-energy XANES region were observed suggesting Co coordination changes in a fraction of the protein (Figs. 3b & 4). **AdoCbl-TsrM** showed increased Co(III) content and the edge shoulder also suggested a base-off cofactor. In contrast, the K-edge shape (small pre-edge feature and shoulder) and energy of the **A3-mutant** suggested stabilization of Co(III) and the predominant presence of a base-on cofactor.

EXAFS simulations using 4 metal-ligand shells and 1 multiple-scattering (ms) contribution provided good fits of all EXAFS spectra (Supplementary Fig. S2; fit error, R_F , ~ 10 %, Supplementary Table 1). The Co-N(corrin) bond lengths (~ 1.88 Å) remained almost unchanged (± 0.02 Å) irrespective of Cbl in solution or bounded to TsrM and of the redox treatments (Supplementary Fig. S2). This reflects the relative stiffness of the Co-corrin geometry and charge delocalization upon Co redox changes. The coordination number (N) of the Co(-N)-C interaction (and the respective ms contribution) provided information on the binding of the nitrogen base (and the nucleotide in AdoCbl) to Co.^[19] For OHCbl- or MeCbl-TsrM, comparably small N-values (9-11) suggested a base-off conformation of the protein-bound cofactor, irrespective of the redox or substrate treatments (Supplementary Fig. S3). The increased N-value for **AdoCbl-TsrM** may be attributed to the binding of the nucleotide at Co (in a base-off conformation). In contrast,

the large N-value in the **A3-mutant** with OHCbl was further consistent with a base-on cofactor conformation.

EXAFS simulation analysis of the 1st-sphere Co-ligand bonds showed that **OHCbl-TsrM** had less than two axial bonds, supporting a base-off cofactor. The shorter and longer distances ($\sim 1.85/2.35$ Å) were attributed to Co(III)-OH and Co(II)-OH₂ bonds, with the latter being more prominent in the DTT-treated sample (Supplementary Fig. S3). **MeCbl-TsrM** treated with DTT showed similar axial ligand parameters as for OHCbl and similar axial bond lengths as MeCbl in solution, in agreement with a base-off cofactor with a methyl group at Co(III). The presence of SAM led to (~ 0.1 Å) elongation of the shorter bond in TsrM with MeCbl vs OHCbl. Further addition of Trp resulted in increased N-values of the axial ligands (in particular for the longer bond), which may be interpreted as reflecting Trp binding at Co (~ 2.3 Å) in addition to a methyl species or more quantitative binding of a Trp vs. a methyl ligand. Interestingly, this result is consistent with the structure of *k_s*TsrM where it was noted that Trp binds partly over the cobalamin cofactor^[13]. The EXAFS parameters for the **A3-mutant** with an N-value close to 2 supported a base-on cofactor and the two bonds were attributed to Co-N(base) (~ 1.85 Å) and Co-OH₂ (~ 2.3 Å) interactions (Supplementary Fig. S3).

Collectively, the XANES and EXAFS data were in perfect agreement with EPR^[18] and structural^[13] analyses of TsrM showing a base-off cobalamin cofactor. In addition, our data establish that substitution of the axial ligand (*i.e.* methyl or adenosine) does not affect the cobalamin binding. However, mutation of the radical SAM cluster changed the cobalamin conformation to base-on, which better preserves the Co(III) state. Finally, spectroscopic analysis also supports that among the B₁₂ analogues tested, MeCbl bound TsrM appears to be more prone to reduction by DTT.

The importance of the base-off conformation is likely to facilitate reduction and methyl transfer to the substrate. Indeed, pentacoordinated alkylcobalamins are strongly destabilized toward heterolysis^[8]. In support of this hypothesis, when we analyzed **OHCbl-TsrM** by UV-visible spectroscopy, we observed that the cobalamin cofactor switched almost instantly from Co(III) ($\lambda_{\text{max}} \sim 350$ nm) to Co(I) ($\lambda_{\text{max}} \sim 390$ nm) under anaerobic conditions after DTT addition (Fig. 5, right panel). In sharp contrast, the **A3-mutant** proved to be hardly reduced even after 90 min incubation (Fig. 5, right panel). Interestingly, a similar result was reported for the corrinoid iron-sulfur protein (CoFeSP), a methyl carrier in the Wood-Ljungdahl pathway of acetyl-CoA synthesis.^[20] However, at odd with CoFeSP, **OHCbl-TsrM** does not require a strong reducing agent to switch to Co(I) and the **A3-mutant** is unable to methylate its substrate.^[20b]

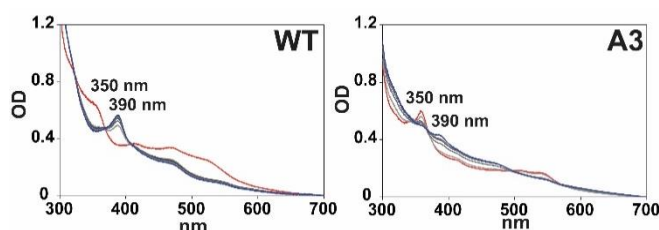


Figure 5. UV-visible analysis of **OHCbl-TsrM** (WT) and **OHCbl-A3-mutant** (A3) reduction after DTT addition. Enzymes (100 μ M) were incubated under anaerobic and reducing conditions after addition of 3 mM DTT. Red traces: as purified enzyme. From grey to blue: reduction of the proteins in the presence of DTT (**WT** from 0 to 30 min, **A3-mutant** from 0 to 90 min).

Probing TsrM substrate promiscuity. In order to trap for reaction intermediates^[7b] or to reorient TsrM catalysis, we prepared a library of tryptophan and tryptamine derivatives^[21] with variations on the amine and/or the ester groups and featuring olefins or propargylamine groups (Fig. 6).

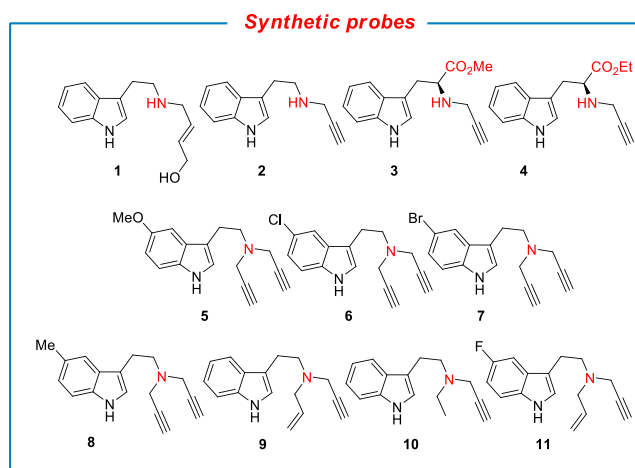


Figure 6. Tryptophan and tryptamine derivatives used as TsrM substrates. See supporting information for synthetic methods.

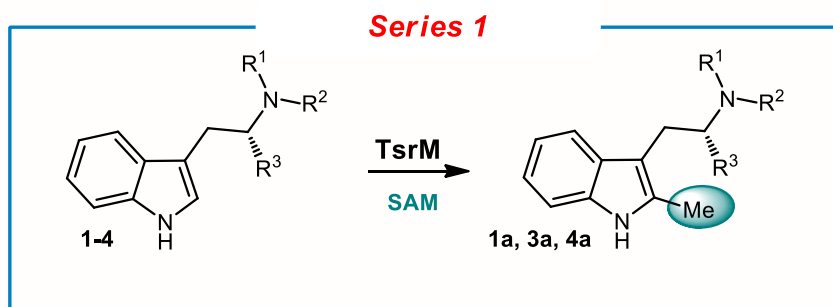
We first incubated **OHCbl-TsrM** with secondary amine (**1-4**) and SAM, under anaerobic and reducing conditions. All these derivatives, except **2**, were enzyme substrates despite the presence of the three or four carbon synthons on the amines (Fig. 6 & 7). We notably obtained a partial conversion of **1** ($[M+H]^+= 231.14$) and full conversion of **3** & **4** ($[M+H]^+= 257.12$ & 271.14) as shown by a mass increment of +14 Da indicating methyl transfer (**1a** $[M+H]^+= 245.16$, **3a** $[M+H]^+= 271.14$ & **4a** $[M+H]^+= 285.16$, Fig. 7 & Supplementary Table 2 & 3, Supplementary Fig. S4). Of note, we did not measure a significant activity difference using as-purified **OHCbl-TsrM** or after anaerobic iron-sulfur reconstitution in-line with the unusual coordination of TsrM iron-sulfur cluster^[13].

To validate the location of the methyl group on the respective products **1a**, **3a** & **4a**, we performed LC-MS/MS analysis (Fig. 7c and Supplementary Fig. S4). As shown with **3a**, several fragments ($[M+H]^+= 216.10$, 174.06 & 146.09) were formed in agreement with TsrM transferring a methyl group on the indole C2 position. To validate this assignment, methyl (*R*)-3-(2-methyl-1H-indol-3-yl)-2-(prop-2-yn-1-ylamino) propanoate **synth-3a** was synthesized (see Supporting information). The LC-MS/MS profile of **synth-3a** and its retention time perfectly superimposed with the product formed with **3** (Supplementary Fig. S5). Finally, when incubating TsrM with **3** in the presence of *d*3-SAM, containing a fully deuterated methyl group, we measured a mass increment of +17 Da which was also localized on the indole moiety of the product ($[M+H]^+= 149.11$) (Fig. 7c, right panel).

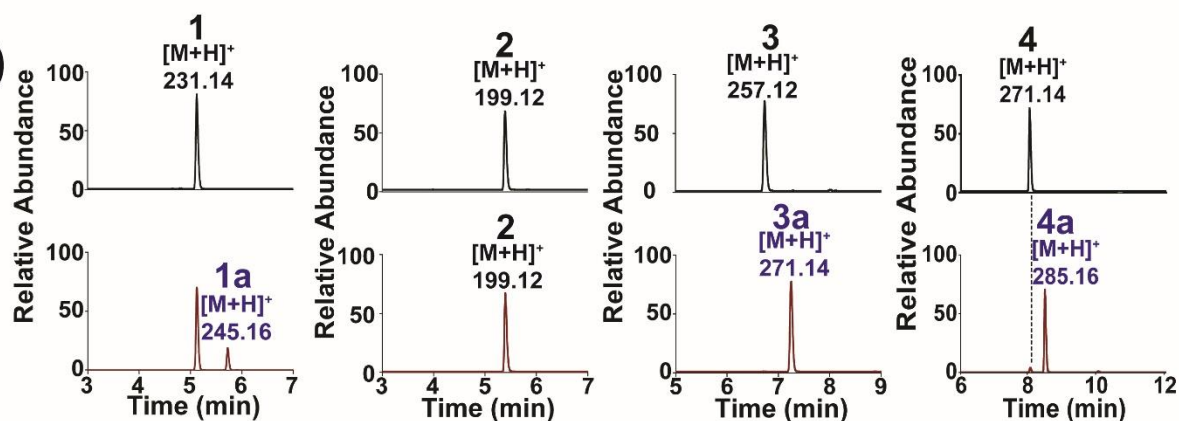
In contrast to the first series, with the di-propargyl derivatives **5-7**, the products formed by TsrM (**5b**, **6b** & **7b**) eluted before the substrate during reversed-phase HPLC-MS analysis indicating a higher polarity than the substrates (Fig. 8). In addition, LC-MS/MS fragmentation patterns of **5b-7b** also strongly differed with formation of a dominant ion fragment corresponding to the indole ring. For instance, with **6** and **6b** the dominant ion was identified as 5-chloro-indolyl ethane ($m/z= 178.04$, Fig. 8 a-c and Supplementary Table 4 & 5) clearly indicating

that a methyl group was not transferred to the indole ring as expected but to the dipropargylamine moiety. Similarly, MS/MS analysis of **5b** & **7b**, showed that a methyl group was transferred to the dipropargylamine moiety with formation of the characteristic fragments corresponding to *N*-methyl-*N,N*-dipropargylamine ($[M+H]^+= 108.08$) and *N*-methyl propargyl fragment ($[M]^+= 68.05$) (Fig. 8c, middle panel & Supplementary Fig. S6). Collectively, these data support that the methyl group was transferred not on a carbon but on the nitrogen atom of these amines, generating *N*-methylammonium species. To definitively support this assignment, we repeated the experiment in the presence of *d*3-SAM (Fig. 8c, right panel & Supplementary Fig. S6). Under these conditions, masses of the *N*-methyl-*N,N*-dipropargylamine and *N*-methyl-*N*-propargylamine moieties shifted by +3 Da ($m/z= 111.10$ & 71.06 , respectively), consistent with the incorporation of a methyl group with three deuterium atoms. We also synthesized authentic *N*-methyl-*N*-(2-(5-chloro-1H-indol-3-yl)ethyl)-*N*-(prop-2-yn-1-yl)prop-2-yn-1-amine (**synth-6b**) by alkylation of **6** with methyl iodide (Supporting information). Not only this compound eluted at the same retention time than **6b** (Supplementary Fig. S7), but its fragmentation pattern was also identical. Finally the structure of **6b** was solved by ¹H-NMR, after preparative enzymatic conversion of **6** and HPLC purification (Fig. 9). Notably, in the aromatic area, characteristic proton chemical shifts confirmed that no substitution occurred on the indole ring and aliphatic protons of **6b** perfectly aligned with the one from **synth-6b**. In addition, incubation of TsrM with **synth-6b** gave no novel product, supporting that it is the only methylated product formed from **6**. Collectively, these results demonstrate that TsrM transfers a methyl group on the dipropargylamine moiety and more importantly, they established that TsrM, instead of catalyzing a C-methyl transfer reaction, is able to catalyze a *N*-methyl transfer reaction.

a



b



c

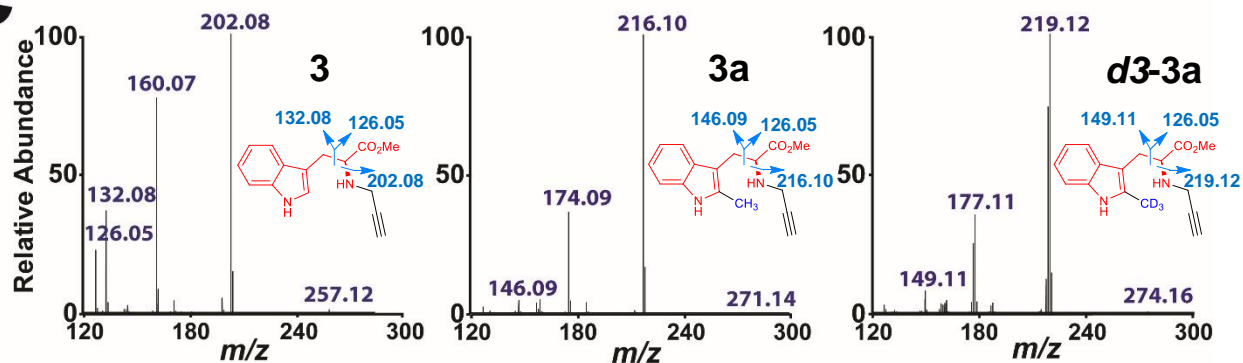


Figure 7. Activity of TsrM on tryptophan and tryptamine derivatives **1-4**. (a) Reaction catalyzed by TsrM on **1-4**. (b) LC-MS analysis of the reactions of TsrM with **1** (m/z = 231.14), **2** (m/z = 199.12), **3** (m/z = 257.12) and **4** (m/z = 271.14). Methylated products (**1a**, **3a** & **4a**) were characterized by a mass shift of Δm = +14 Da. (c) LC-MS/MS analysis of **3** (left panel) and the reaction product **3a** after incubation with TsrM under anaerobic conditions in the presence of SAM (middle panel, **3a**) or d3-SAM (right panel, **d3-3a**).

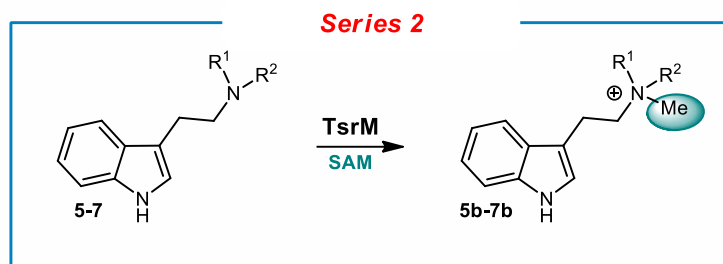
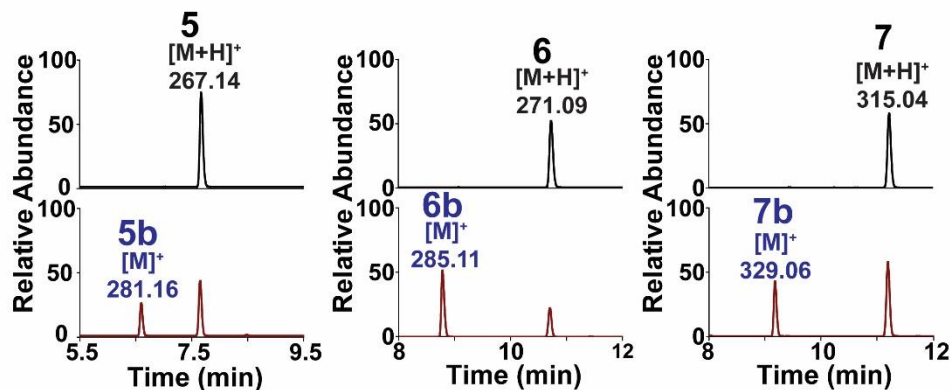
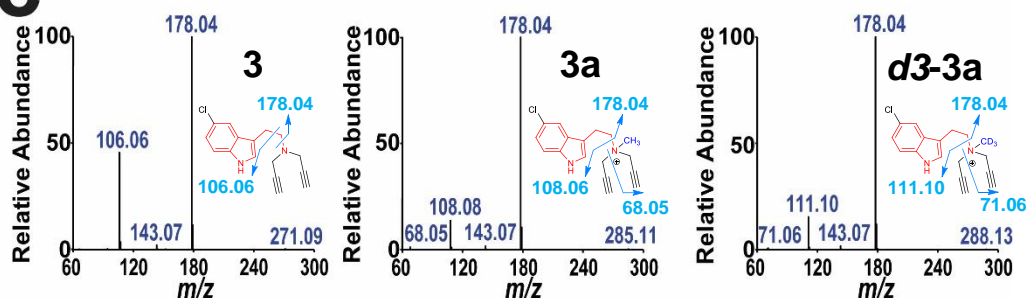
a**b****c**

Figure 8. Activity of TsrM on tryptamine di-propargyl derivatives. (a) Reaction catalyzed by TsrM on **5-7**. (b) LC-MS analysis of the reactions of TsrM with **5** (m/z = 267.14), **6** (m/z = 271.09) and **7** (m/z = 315.04). Methylated products **5b**, **6b** & **7b** were characterized by a mass shift of Δm = 14 Da. (c) LC-MS/MS analysis of **6** (left panel) and the reaction product **6b** obtained in the presence of SAM (middle panel) or d3-SAM (right panel).

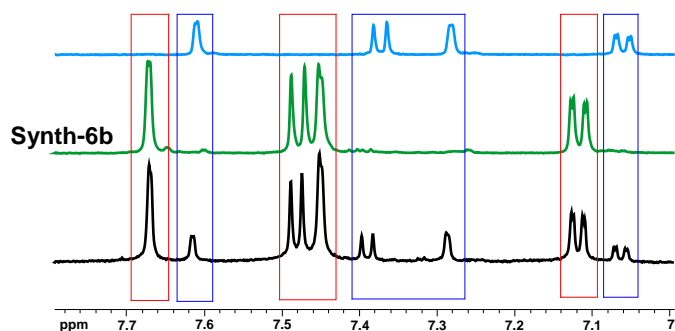


Figure 9. ^1H -NMR analysis of **6** (blue trace), **synth-6b** (green trace) and the reaction mixture **6** and **6b** (black trace) obtained after incubation of **6** with TsrM and SAM. See (Supplementary Fig. S8) for assignment.

With the *N,N*-disubstituted tryptamines **8-11**, we systematically obtained two methylated products. LC-MS/MS analysis was consistent

with the product with the higher polarity being methylated on the *N,N*-dipropargylamine moiety while the product eluting after the substrate was methylated on the indole ring, as shown for **1**, **3** & **4** (Supplementary Fig. S9). In addition, we also obtained bis-methylated products with **8** and **9** (**8c**, m/z = 279.18, **9c**, m/z = 267.18), which fragmentation spectra indicated that methylation occurred on both the indole and the *N,N*-dipropargylamine moieties (Fig. 10b). Consistent with this analysis, incubation of **8** with TsrM and d3-SAM produced a bis-methylated product with a +34 Da mass increment, demonstrating that two CD_3 groups were transferred from d3-SAM to **d6-8c** (Supplementary Fig. S10).

To obtain a better picture of TsrM methylation capacity, we performed prolonged incubation with **3**, **6** and **8** (Fig. 10c). As shown, we were able to obtain >70% conversion of mono-methylated products **3a**, **6b**, **8a** & **8b** but only **8** gave a di-methylated product **8c**.

Incubation with the **A3-mutant**, despite the presence of SAM and bound cobalamin, never led to the formation of methylated product while we observed SAH formation (**Fig. 10c & Supplementary Fig. S11**), further demonstrating that the C- and N-methylation activities observed, are genuine TsrM activities. Kinetic analysis of the reactions catalyzed by TsrM, showed a stoichiometric relation between SAH production and methylated product (**Fig. 10d**). Reaction rate for the formation of the C2-methyl-indole derivatives **3a** and **8a** ($2.17 \mu\text{mol} \cdot \text{min}^{-1}$ & $0.24 \mu\text{mol} \cdot \text{min}^{-1}$, respectively) or the N-methyl derivatives **6b** & **8b** ($0.27 \mu\text{mol} \cdot \text{min}^{-1}$ and $0.09 \mu\text{mol} \cdot \text{min}^{-1}$, respectively) greatly differed depending on the substrate assayed. However, methylation on the indole ring was generally faster (**Fig. 10d**).

C4-methylation catalyzed by TsrM. Since TsrM was able to introduce several methyl groups on synthetic substrates, we carefully investigated its activity with Trp. We notably noticed the formation of one additional product eluting after 2Me-Trp at ~ 24.5 min and sharing the same UV and fluorescence properties than Trp (**Fig. 11**). LC-MS analysis of this compound indicated that it was a di-methylated product ($[\text{M}+\text{H}]^+$: 233). Since this product accumulated after Trp consumption, we hypothesized that it was a 2Me-Trp derivative. To confirm this hypothesis, we synthesized 2Me-Trp using tryptophan synthase as recently described^[21a] and used it as substrate. Surprisingly, 2Me-Trp proved to be a substrate for TsrM albeit with a reduced activity (**Supplementary Fig. S12**). With 2Me-Trp, we obtained a dimethylated product eluting at the same retention time than the dimethylated product formed with Trp. NMR analysis of the reaction (**Fig. 11c**) identified this novel product as 2,4-dimethyl-Trp, based notably on the characteristic H5, H6 & H7 chemical shifts and the concomitant disappearing of the H4 signal. NMR analysis also indicated that other di- and trimethylated products were formed during catalysis, a result confirmed by LC-MS analysis (**Supplementary Fig. S13**). To further validate this structural assignment, we incubated TsrM with 4Me-Trp and obtained a dimethylated product that eluted at the same retention time than 2,4-dimethyl-Trp (**Fig. 11**). Thus TsrM, is able not only to install methylation on C2 but also on the C4 position, the least reactive position of Trp.

To further explore the influence of Trp substitutions on TsrM activity, we incubated the enzyme with the racemic tryptophan derivatives **12**, **13**, **14** & **15**, substituted on the C4, C5, C6 and C7 positions, respectively (**Fig. 12**). As shown, with the exception of 1-Me-Trp which was a known enzyme inhibitor^[7b], all the compounds assayed were enzyme substrates leading to the formation of a wide range of di-, tri- and tetra-methylated products (**Fig. 12**). By using TsrM and tryptophan synthase^[21a], we accessed 18 references compounds including 2,4-, 2,5-, 1,2-dimethyltryptophan as well as 2-methyltryptophan-methylester and N-methyl, 2-methyltryptophan (**Supplementary Table 6**).

With **12**, **13**, **14** & **15**, we obtained one major product that we assigned as 2,4-, 2,5-, 2,6- & 2,7-dimethyl-Trp, respectively, based on their retention time (**Supplementary Table 6**), fragmentation patterns (**Supplementary Fig. S14**) and NMR analysis (**Supplementary Fig. S15**). Interestingly, when the incubation proceeded, other products accumulated notably tri and tetramethylated products (*i.e.* two and three methylation events).

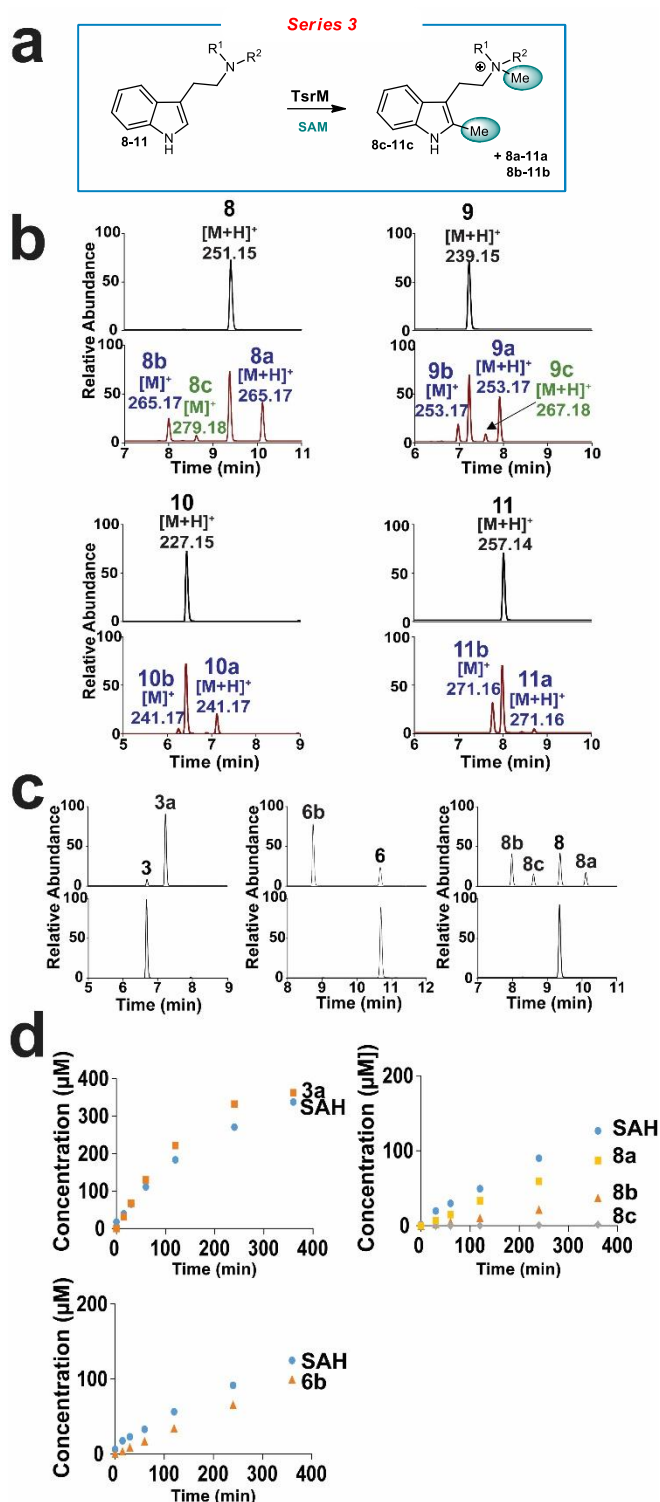


Figure 10. Activity of TsrM on tryptamine derivatives. (a) Reaction catalyzed by TsrM on **8-11**. (b) LC-MS analysis of the reactions of TsrM with **8** ($m/z = 251.15$), **9** ($m/z = 239.15$), **10** ($m/z = 227.15$) and **11** ($m/z = 257.14$). Methylated products were characterized by a mass shift of $\Delta m = +14$ Da, while di-methylated products were characterized by a mass shift of $\Delta m = +28$ Da. (c) LC-MS analysis of TsrM (upper traces) and the **A3-mutant** (lower traces) incubated with **3**, **6** or **8** under anaerobic and reducing conditions in the presence of SAM after 72 hours incubation. (d) Kinetic analysis of the reaction of TsrM with **3** (Upper left panel), **8** (Upper right panel) and **6** (Lower left panel). Symbols are as follows: \bullet : SAH; \blacksquare : methylated product on the indole ring; \blacktriangle : N-methylation on the propargylamine moiety; \blacklozenge : bismethylated product.

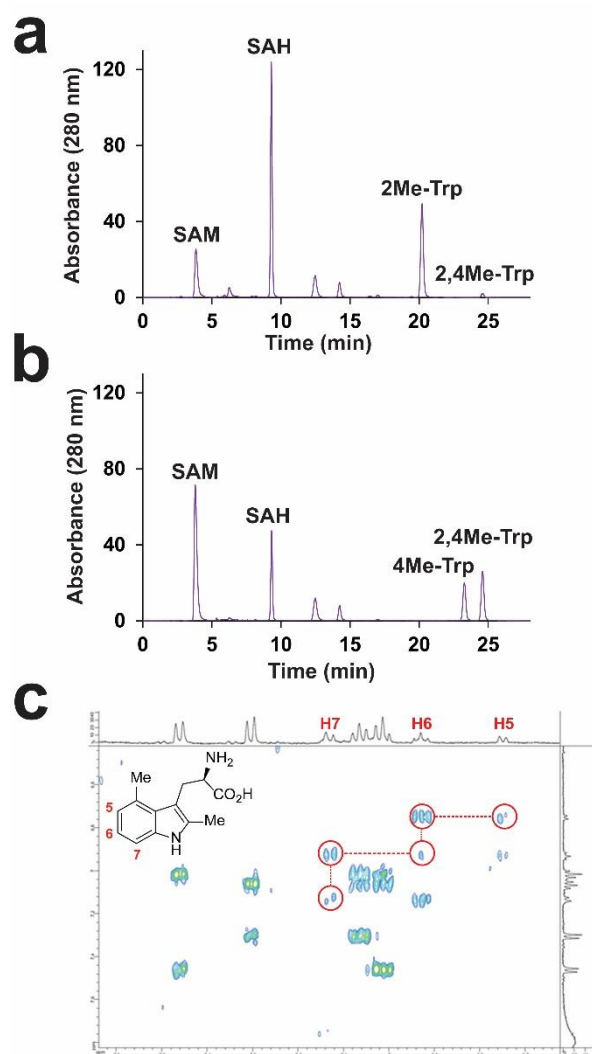


Figure 11. Production of 2,4 dimethyl-Trp by TsrM. (a) HPLC analysis of an overnight incubation of TsrM with Trp leading to the production of SAH, 2Me-Trp and low amount of a 2,4-dimethyl-Trp. (b) HPLC analysis of an overnight incubation of TsrM with 4Me-Trp. UV detection at 278 nm. (c) NMR analysis of 2,4-dimethyl-Trp produced by TsrM.

This was particularly evident with **13** and **15** for which the dimethylated products (2,5- and 2,7-dimethyl-Trp) were almost completely converted into tri- and tetramethylated products (**Fig. 12 & Supplementary Fig. S15**), with one assigned as 2,4,7-trimethyl-tryptophan (**Supplementary Fig. S15**). Incubation of these substrates with the A3-mutant, even after extended period of time, never led the formation of any alkylated product.

Altogether, these results demonstrate that TsrM activity is not restricted to the 2 position. They also establish that TsrM can surprisingly catalyze multiple alkylation events even on its product 2Me-Trp. Remarkably, with **13** and **15**, these multi-alkylated products were the major products formed.

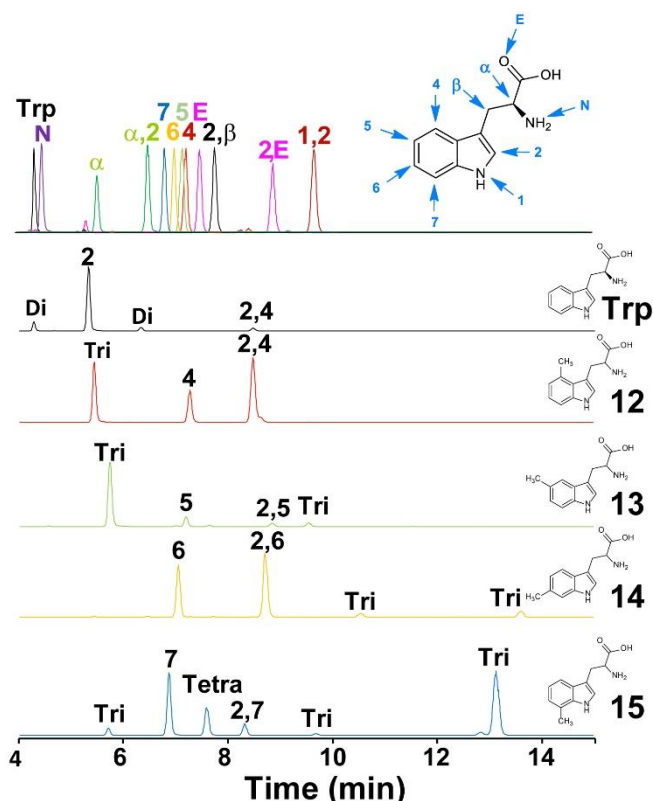


Figure 12. Activity of TsrM on Trp and methyl-tryptophans **12**, **13**, **14** & **15** analysed by LC-MS. Upper trace: reference compounds. Letters and numbers indicate location of methyl groups. E indicates tryptophan methylester. N: N-methyl tryptophan. Di: Dimethylated-Trp. Tri: Trimethylated-Trp. Tetra: Tetramethylated-Trp. Substrates (Trp, **12**, **13**, **14** & **15**) were incubated overnight with TsrM and SAM under anaerobic and reducing conditions.

Discussion

The reaction mechanism of TsrM, a B₁₂-dependent radical SAM enzyme has been controversial since its discovery almost ten years ago.^[7c] Indeed, early studies have shown that, unlike all other known radical SAM enzymes, TsrM does not require an external electron source and does not homolytically cleave SAM^[7b, 7c] questioning the radical nature of its mechanism. Thanks to the development of synthetic probes, we unambiguously demonstrate that TsrM is indeed able to catalyze nucleophilic reactions (**Fig. 6-8**). Equally important, we show that it is possible to turn this C-methyl transferase into an N-methyl transferase, allowing access to the synthesis of a diversity of methyl tryptophan and tryptamine derivatives (**Fig. 14**). To the best of our knowledge, this is the first example of a C-methyltransferase catalyzing methyl transfer on nucleophilic heteroatoms.

Another surprising result was the ability of TsrM to not only install methyl groups on propargyl moieties but also to catalyze methyl transfer on other positions of the indole ring, notably the C4, which is the less reactive position. Probably, the most notorious example of Trp alkylation on C4, is the one catalyzed by prenyltransferases^[22]. These enzymes generate a dimethylallyl carbocation that reacts in an electrophilic aromatic substitution at the indole ring. Such chemically challenging substitution likely occurs via a C3-substitution followed by a Cope rearrangement, which is far from a direct functionalization.^[23] Another well-known aromatic alkyltransferase is CouO which catalyzes a Friedel–Crafts alkylation on various substrates such as naphthalene^[24]. However, its mechanism involves the essential deprotonation of one hydroxyl group, adjacent to the alkylation site, in order to generate a

resonance stabilized phenolate. Thus, the ability of TsrM to catalyze direct methyl transfer at different locations of the indole ring (the benzyl and the pyrrole moieties), independently of their nucleophilicity, is unique. The recent structural study of k_s TsrM in complex with Trp has shown that only the C7 was at a reasonable distance from MeCbl (3.1 Å) for methyl transfer, suggesting that Trp was in “flipped conformation”^[13]. Our data support that Trp in fact, can adopt different functional conformations in TsrM active site, supporting catalysis and the installation of methyl group on different positions.

Another intriguing feature of k_s TsrM is that the radical SAM cluster is fully ligated by three Cys residues and a Glu residue (**E273**). This has been proposed to preclude SAM binding to the cluster and hence its radical cleavage. However, coordination of the [4Fe4S] cluster by **E273** could also represent an intermediate state, as recently shown for another enzyme, Mmp10^[8]. In order to test this hypothesis, we cloned and expressed k_s TsrM and performed site directed mutagenesis to replace **E273** by an Ala residue. Interestingly, this mutant was severely impaired for 2Me-Trp production (**Fig. 13**). In addition, even in the presence of sodium dithionite or other reductants, it was unable to cleave SAM supporting that this residue is important but that other factors prevent TsrM from catalyzing the radical cleavage of SAM (**Fig. 13**).

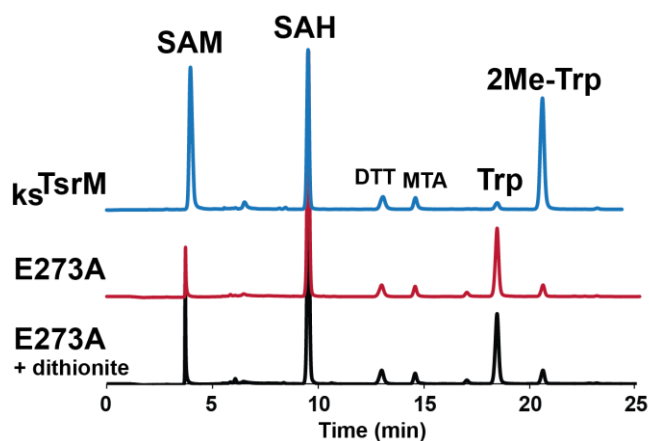
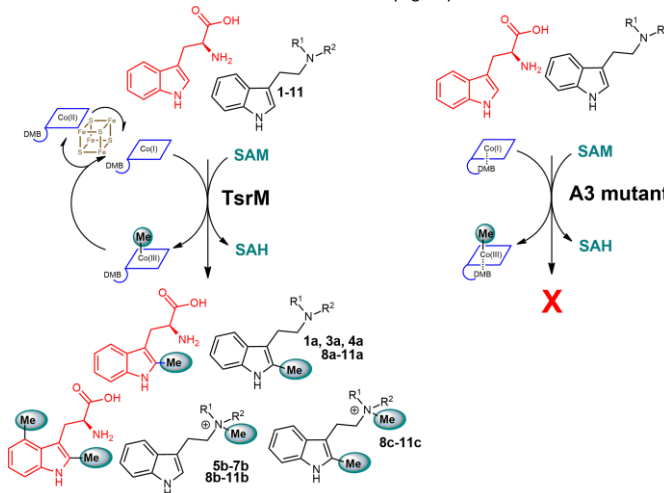


Figure 13. Activity of k_s TsrM and the E273A mutant on Trp. Upper trace: wild-type k_s TsrM. Middle trace: E273A mutant. Lower trace: E273A mutant incubated with dithionite. HPLC analysis with UV (278nm) monitoring.

As shown previously^[7b] and hereby, the radical SAM cluster is essential for TsrM activity but its role is still unclear. XAS analysis suggests that the cobalamin cofactor switches from a base-off in the wild-type enzyme to a base-on cofactor in the **A3-mutant**. This likely reflects an important role of the radical SAM domain for the proper pentacoordination of the cobalamin cofactor, which is critical for the reactivity of the C-Co bond. We have shown here by UV-visible analysis that **OHCbl-TsrM** (**Fig. 5**) is easily reduced from Co(III) to Co(I) upon DTT addition while the **A3-mutant** is barely reducible under the same conditions. A similar result was reported for the CoFeSP^[20b]. However, this enzyme like the B₁₂-dependent methionine synthase,^[16b, 25] requires a stronger reductant (e.g. Ti(III)Citrate) for reduction, in sharp contrast to TsrM.^[20b] Intriguingly, after reduction, the Co(I) state of TsrM is particularly stable, a property shared by at least one other B₁₂-dependent enzyme^[26]. Thus, the radical [4Fe-4S] cluster likely participates to the stabilization of the cobalamin base-off cofactor, but its role as an electron conduit for the cobalamin cofactor remains to be fully investigated.

Figure 14. Reaction catalyzed by TsrM on tryptophan and tryptamine derivatives 8-11. With **1-4** only C2-methyl-indole derivatives were obtained while with **5-7** methylation occurred on the *N*-propargylamine function. Derivatives **8-11** gave bismethylated products. With Trp, not only methylation on the C2 but also the C4 occurred. The wild-type TsrM likely transfers a methyl group from a base-off Co(III) methyl-cobalamin, cycling from Co(III) to Co(I). The FeS-cluster plays a critical role for the conformation of the cobalamin cofactor and transfer of the methyl group to the substrate. The **A3-**



mutant, lacking the radical SAM cluster, despite being able to transfer a methyl group from SAM to cobalamin, has a base-on cofactor and is not able to transfer the methyl group to any substrate.

Conclusion

Our study reveals that TsrM, in addition to catalyzing the alkylation of the electron rich C2 of Trp, can also alkylate the most challenging position of the indole ring (*i.e.* C4 position) likely *via* a direct methyl transfer reaction (**Fig. 14**). It is intriguing that such reaction could occur without the requirement of a carbanion intermediate^[27], intermediate stabilization^[24] or secondary rearrangement^[23]. Interestingly, TsrM can introduce multiple methyl groups on its substrate despite the distinct reactivity of the carbon-atoms in the indole ring. Under our experimental conditions, up to three methyl groups were installed on Trp and modification of the alkyl chain, independently of the presence of an electron-donating or electron-withdrawing group, strongly orient the nature of the products formed leading to a diversity of C- and N-methylated products.

TsrM has indeed the remarkable property to transfer methyl groups on nucleophilic atoms demonstrating that it is able to catalyze methyl transfer reaction *via* a polar mechanism (**Fig. 14**). Other radical SAM enzymes such as Cfr^[28], MiaB^[29] and QueE^[30] have been proposed to employ SAM as a polar cofactor in their respective reactions. However, in contrast to TsrM, all these enzymes require an external electron donor for catalysis. Collectively, our study demonstrates that TsrM catalyzes non-radical reactions and is a unique versatile alkylating agent able to functionalize chemically challenging carbon-atoms and to catalyze multiple alkylation events, expanding the catalytic versatility of radical SAM enzymes^[8] and giving an easy access to various chemical syntheses. However, questions remain regarding the mechanism of this intriguing enzyme notably how it can catalyze direct methyl transfer reaction to unreactive carbon-atoms.

Acknowledgements

This work was supported by the European Research Council (ERC consolidator grant 617053), ANR (grants ANR-17-CE11-0014 & ANR-20-CE07-0037 BiAuCat) and the CHARMMMAT Laboratory of Excellence (No. ANR-11-LABX0039).

- [1] a) A. Benjdia, O. Berteau, *Front Chem* **2021**, *9*, 678068; b) A. Benjdia, C. Balty, O. Berteau, *Front Chem* **2017**, *5*, 87; c) N. Mahanta, G. A. Hudson, D. A. Mitchell, *Biochemistry* **2017**, *56*, 5229-5524.
- [2] a) P. G. Arnison, M. J. Bibb, G. Bierbaum, A. A. Bowers, T. S. Bugni, G. Bulaj, J. A. Camarero, D. J. Campopiano, G. L. Challis, J. Clardy, P. D. Cotter, D. J. Craik, M. Dawson, E. Dittmann, S. Donadio, P. C. Dorrestein, K. D. Entian, M. A. Fischbach, J. S. Garavelli, U. Goransson, C. W. Gruber, D. H. Haft, T. K. Hemscheidt, C. Hertweck, C. Hill, A. R. Horswill, M. Jaspars, W. L. Kelly, J. P. Klinman, O. P. Kuipers, A. J. Link, W. Liu, M. A. Marahiel, D. A. Mitchell, G. N. Moll, B. S. Moore, R. Muller, S. K. Nair, I. F. Nes, G. E. Norris, B. M. Olivera, H. Onaka, M. L. Patchett, J. Piel, M. J. Reaney, S. Rebuffat, R. P. Ross, H. G. Sahl, E. W. Schmidt, M. E. Selsted, K. Severinov, B. Shen, K. Sivonen, L. Smith, T. Stein, R. D. Sussmuth, J. R. Tagg, G. L. Tang, A. W. Truman, J. C. Vederas, C. T. Walsh, J. D. Walton, S. C. Wenzel, J. M. Willey, W. A. van der Donk, *Nat. Prod. Rep.* **2013**, *30*, 108-160; b) C. Balty, A. Guillot, L. Fradale, C. Brewee, M. Boulay, X. Kubiak, A. Benjdia, O. Berteau, *J Biol Chem* **2019**, *294*, 14512-14525; c) C. Balty, A. Guillot, L. Fradale, C. Brewee, B. Lefranc, C. Herrero, C. Sandström, J. Leprince, O. Berteau, A. Benjdia, *J Biol Chem* **2020**, *295*, 16665-16677; d) A. Benjdia, A. Guillot, P. Ruffié, J. Leprince, O. Berteau, *Nat Chem* **2017**, *9*, 698-707; e) N. Mahanta, Z. Zhang, G. A. Hudson, W. A. van der Donk, D. A. Mitchell, *J Am Chem Soc* **2017**, *139*, 4310-4313; f) G. A. Hudson, B. J. Burkhart, A. J. DiCaprio, C. Schwalen, B. Kille, T. V. Pogorelov, D. A. Mitchell, *J. Am. Chem. Soc.* **2019**; g) J. W. LaMattina, B. Wang, E. D. Badding, L. K. Gadsby, T. L. Grove, S. J. Booker, *J Am Chem Soc* **2017**, *139*, 17438-17445.
- [3] a) M. F. Freeman, C. Gurgui, M. J. Helf, B. I. Morinaka, A. R. Uriá, N. J. Oldham, H. G. Sahl, S. Matsunaga, J. Piel, *Science* **2012**, *338*, 387-390; b) P. F. Popp, A. Benjdia, H. Strahl, O. Berteau, T. Mascher, *Front Microbiol* **2020**, *11*, 151; c) P. F. Popp, L. Friebe, A. Benjdia, A. Guillot, O. Berteau, T. Mascher, *Microb Physiol* **2021**, 1-12.
- [4] B. Khaliullin, R. Ayikpoe, M. Tuttle, J. A. Latham, *J Biol Chem* **2017**, *292*, 13022-13033.
- [5] a) K. R. Schramma, L. B. Bushin, M. R. Seyedsayamdost, *Nat. Chem.* **2015**, *7*, 431-437; b) A. Benjdia, L. Decamps, A. Guillot, X. Kubiak, P. Ruffie, C. Sandstrom, O. Berteau, *J Biol Chem* **2017**, *292*, 10835-10844; c) L. Tao, W. Zhu, J. P. Klinman, R. D. Britt, *Biochemistry* **2019**, *58*, 5173-5187; d) I. Barr, J. A. Latham, A. T. Iavarone, T. Chantarojsiri, J. D. Hwang, J. P. Klinman, *J Biol Chem* **2016**, *291*, 8877-8884.
- [6] a) L. K. Flühe, T. A.; Gattner, M. J.; Schäfer, A.; Burghaus, O.; Linne, U.; Marahiel, M. A., *Nat. Chem. Biol.* **2012**, *8*, 350-357; b) A. Benjdia, A. Guillot, B. Lefranc, H. Vaudry, J. Leprince, O. Berteau, *Chem Commun (Camb)* **2016**, *52*, 6249-6252; c) N. A. Bruender, J. Wilcoxon, R. D. Britt, V. Bandarian, *Biochemistry* **2016**, *55*, 2122-2134.
- [7] a) A. Parent, A. Guillot, A. Benjdia, G. Chartier, J. Leprince, O. Berteau, *J Am Chem Soc* **2016**, *138*, 15515-15518; b) A. Benjdia, S. Pierre, C. Gherasim, A. Guillot, M. Carmona, P. Amara, R. Banerjee, O. Berteau, *Nat Commun* **2015**, *6*, 8377; c) S. Pierre, A. Guillot, A. Benjdia, C. Sandstrom, P. Langella, O. Berteau, *Nat Chem Biol* **2012**, *8*, 957-959.
- [8] C. D. Fyfe, N. Bernardo-Garcia, L. Fradale, S. Grimaldi, A. Guillot, C. Brewee, L. M. G. Chavas, P. Legrand, A. Benjdia, O. Berteau, *Nature* **2022**, *602*, 336-342.
- [9] W. J. Werner, K. D. Allen, K. Hu, G. L. Helms, B. S. Chen, S. C. Wang, *Biochemistry* **2011**, *50*, 8986-8988.
- [10] a) J. Bridwell-Rabb, A. Zhong, H. G. Sun, C. L. Drennan, H. W. Liu, *Nature* **2017**, *544*, 322-326; b) Z. M. Yang, C. E. Bauer, *J Bacteriol* **1990**, *172*, 5001-5010; cA. Zhong, Y. H. Lee, Y. N. Liu, H. W. Liu, *Biochemistry* **2021**, *60*, 537-546.
- [11] a) D. R. Marous, E. P. Lloyd, A. R. Buller, K. A. Moshos, T. L. Grove, A. J. Blaszczyk, S. J. Booker, C. A. Townsend, *Proc Natl Acad Sci U S A* **2015**, *112*, 10354-10358; b) H. J. Kim, Y. N. Liu, R. M. McCarty, H. W. Liu, *J Am Chem Soc* **2017**, *139*, 16084-16087; c) M. I. McLaughlin, K. Pallitsch, G. Wallner, W. A. van der Donk, F. Hammerschmidt, *Biochemistry* **2021**, *60*, 1587-1596; d) Y. Wang, T. P. Begley, *J Am Chem Soc* **2020**, *142*, 9944-9954; e) Y. Wang, B. Schnell, S. Baumann, R. Muller, T. P. Begley, *J Am Chem Soc* **2017**, *139*, 1742-1745; f) D. Deobald, L. Adrian, C. Schone, M. Rother, G. Layer, *Sci Rep* **2018**, *8*, 7404.
- [12] a) W. L. Kelly, L. Pan, C. Li, *J Am Chem Soc* **2009**, *131*, 4327-4334; b) L. Duan, S. Wang, R. Liao, W. Liu, *Chem Biol* **2012**, *19*, 443-448.
- [13] H. L. Knox, P. Y. Chen, A. J. Blaszczyk, A. Mukherjee, T. L. Grove, E. L. Schwalm, B. Wang, C. L. Drennan, S. J. Booker, *Nat Chem Biol* **2021**, *17*, 485-491.
- [14] P. J. Gritsch, C. Leitner, M. Pfaffenbach, T. Gaich, *Angew Chem Int Ed Engl* **2014**, *53*, 1208-1217.
- [15] L. M. Alkhalaf, K. S. Ryan, *Chem Biol* **2015**, *22*, 317-328.
- [16] a) J. C. Escalante-Semerena, M. J. Warren, *EcoSal Plus* **2008**, *3*; b) R. G. Matthews, M. Koutmos, S. Datta, *Curr Opin Struct Biol* **2008**, *18*, 658-666.
- [17] N. D. Lanz, A. J. Blaszczyk, E. L. McCarthy, B. Wang, R. X. Wang, B. S. Jones, S. J. Booker, *Biochemistry* **2018**, *57*, 1475-1490.
- [18] A. J. Blaszczyk, A. Silakov, B. Zhang, S. J. Maiocco, N. D. Lanz, W. L. Kelly, S. J. Elliott, C. Krebs, S. J. Booker, *J Am Chem Soc* **2016**, *138*, 3416-3426.
- [19] P. Schrapers, S. Mebs, S. Goetzl, S. E. Hennig, H. Dau, H. Dobbek, M. Haumann, *PLoS One* **2016**, *11*, e0158681.
- [20] a) Y. Kung, N. Ando, T. I. Doukov, L. C. Blasiak, G. Bender, J. Seravalli, S. W. Ragsdale, C. L. Drennan, *Nature* **2012**, *484*, 265-269; b) S. Menon, S. W. Ragsdale, *Biochemistry* **1998**, *37*, 5689-5698.
- [21] a) N. Sabat, F. Soualmia, P. Retailleau, A. Benjdia, O. Berteau, X. Guinchard, *Org Lett* **2020**, *22*, 4344-4349; b) V. Gobé, P. Retailleau, X. Guinchard, *Chem. Eur. J.* **2015**, *21*, 17587-17590; c) V. Magné, A. Marinetti, V. Gandon, A. Voituriez, X. Guinchard, *Adv. Synth. Catal.* **2017**, *359*, 4036-4042.
- [22] L. Y. Luk, Q. Qian, M. E. Tanner, *J Am Chem Soc* **2011**, *133*, 12342-12345.
- [23] D. D. Schwarzer, P. J. Gritsch, T. Gaich, *Angew Chem Int Ed Engl* **2012**, *51*, 11514-11516.
- [24] H. Stecher, M. Teng, B. J. Ueberbacher, P. Remler, H. Schwab, H. Griengl, M. Gruber-Khadjawi, *Angew Chem Int Ed Engl* **2009**, *48*, 9546-9548.
- [25] R. V. Banerjee, R. G. Matthews, *FASEB J* **1990**, *4*, 1450-1459.
- [26] Z. Li, N. A. Lesniak, R. Banerjee, *J Am Chem Soc* **2014**, *136*, 16108-16111.
- [27] P. Weigle, E. A. Raleigh, *Chem Rev* **2016**, *116*, 12655-12687.
- [28] T. L. Grove, J. S. Benner, M. I. Radle, J. H. Ahlum, B. J. Landgraf, C. Krebs, S. J. Booker, *Science* **2011**, *332*, 604-607.
- [29] a) B. Zhang, A. J. Arcinas, M. I. Radle, A. Silakov, S. J. Booker, C. Krebs, *J Am Chem Soc* **2020**, *142*, 1911-1924; b) F. Pierrel, H. L. Hernandez, M. K. Johnson, M. Fontecave, M. Atta, *J Biol Chem* **2003**, *278*, 29515-29524.
- [30] N. A. Bruender, T. A. Grell, D. P. Dowling, R. M. McCarty, C. L. Drennan, V. Bandarian, *J Am Chem Soc* **2017**, *139*, 1912-1920.

